



Measurements of the $t\bar{t}$ Cross Section in the lepton+jets Channel with 4.3 fb^{-1}

The D0 Collaboration
URL <http://www-d0.fnal.gov>
(Dated: May 28, 2010)

We present a measurement of the inclusive $t\bar{t}$ pair production cross section in $p\bar{p}$ collisions at $\sqrt{s} = 1.96 \text{ TeV}$ utilizing 4.3 fb^{-1} of data collected with the D0 detector at the Fermilab Tevatron Collider. We consider final states containing one high- p_T electron or muon and at least two jets. We perform two analyses, one exploiting specific kinematic features of $t\bar{t}$ events, the other using b -jet identification to separate $t\bar{t}$ signal from background and extract the cross section. For a top quark mass of 172.5 GeV , we obtain $\sigma_{t\bar{t}} = 7.70_{-0.70}^{+0.79}$ (stat + syst + lumi) pb using purely kinematic information and $\sigma_{t\bar{t}} = 7.93_{-0.91}^{+1.04}$ (stat + syst + lumi) pb using b -jet identification to separate signal from background.

Preliminary Results for Summer 2010 Conferences

I. INTRODUCTION

The top quark pair production cross section $\sigma_{t\bar{t}}$ is known with a precision of $\approx 6 - 8\%$ in the standard model (SM) for a given top quark mass [1–3]. Any deviation of its measured value from the SM prediction could signal the presence of new physics in top-pair production or $t\bar{t}$ decays. For example, the decay of a top quark into a charged Higgs boson and a b -quark ($t \rightarrow H^+ b$) would affect the measured value of $\sigma_{t\bar{t}}$ extracted in individual final states relative to the SM prediction. In this analysis, we measure the $t\bar{t}$ production cross section in lepton+jets channels using two different methods, a “kinematical” method based on event kinematics and a counting method using b -jet identification.

II. D0 DETECTOR

The D0 detector contains a tracking system, calorimeter, and a muon spectrometer [4]. The tracking system consists of a silicon microstrip tracker (SMT) and a central fiber tracker (CFT), both located inside a 1.9 T superconducting solenoid. The tracker design provides efficient charged particle measurements in the pseudorapidity [5] region $|\eta| < 3$. The SMT strip pitch of 50–80 μm provides a capability to reconstruct the primary interaction vertex (PV) with a precision of about 40 μm in the plane transverse to the beam direction, dominated by the beam spot size of 30 μm , and a determination of the impact parameter of any tracky relative to the PV [6] with a precision between 20 and 50 μm depending on the number of SMT hits, which are the key components of lifetime-based b -jet tagging. The calorimeter has a central section (CC) covering $|\eta| < 1.1$, and two end calorimeters (EC) extending the coverage to $|\eta| \approx 4.2$. The muon system surrounds the calorimeter and consists of three layers of tracking detectors and two layers of scintillators [7] covering $|\eta| < 2$. A 1.8 T toroidal iron magnet is located outside the innermost layer of the muon detector. The luminosity is calculated from the rate for $p\bar{p}$ inelastic collisions detected with plastic scintillator arrays placed in front of the EC cryostats.

III. EVENT SELECTION

The current measurement is based on data collected with the D0 detector at the Fermilab Tevatron $p\bar{p}$ collider at $\sqrt{s} = 1.96$ TeV, and corresponds to an integrated luminosity of $4.3 \pm 0.3 \text{ fb}^{-1}$, a factor of four greater than that of our previous measurement [8]. The data was taken during the Run II phase of D0 operation. The analysis uses the decay channel $t\bar{t} \rightarrow W^+ b W^- \bar{b}$. W bosons can decay hadronically into $q\bar{q}'$ pairs or leptonically into $e\nu_e$, $\mu\nu_\mu$, and $\tau\nu_\tau$. If one of the W bosons decays hadronically while the other one produces a direct electron or muon or a secondary electron or muon from τ decay, the final state is referred to as the lepton+jets (ℓ +jets) channel. If both W bosons decay leptonically, this leads to a dilepton final state containing a pair of electrons, a pair of muons, or an electron and a muon. Hadronically decaying tau leptons are not identified here. The $t\bar{t}$ production process where both W bosons decay hadronically is not considered here.

To select events in the ℓ +jets channels, the trigger requires at least one electron or an electron and a jet for the e +jets channel, and at least one muon for the μ +jets final state. We enrich the $t\bar{t}$ component by requiring ≥ 2 jets with transverse momentum $p_T > 20$ GeV and pseudorapidity $|\eta| < 2.5$. Furthermore, we require one isolated electron with $p_T > 20$ GeV and $|\eta| < 1.1$, or one isolated muon with $p_T > 20$ GeV and $|\eta| < 2.0$, and missing transverse energy $\cancel{E}_T > 20(25)$ GeV in the e +jets (μ +jets) channel. Additionally, the highest p_T jet is required to have $p_T > 40$ GeV. Events containing a second isolated electron or muon with $p_T > 15$ GeV are rejected. The lepton isolation criteria are based on calorimeter and tracking information. Details of lepton, jets and \cancel{E}_T identification are described elsewhere [9]. We identify b -jets using a neural-network b -tagging algorithm [10]. It combines variables that characterize the presence and properties of secondary vertices and tracks inside the jet with high impact parameter relative to the PV.

We split the selected ℓ +jets sample into subsamples according to lepton flavor (e or μ) and jet multiplicity. For the measurement where we do not apply b -tagging, we use 2, 3 or ≥ 4 jets final states defining six separate data sets. We form a discriminant \mathcal{D} that exploits kinematic differences between the background and $t\bar{t}$ signal. For the measurement including b -tagging we require at least three jets and split data into additional subsamples according to the number of tagged b -jet candidates (0, 1 or ≥ 2), thus obtaining twelve separate data sets.

IV. SAMPLE COMPOSITION

After event selection, the sample consists of signal and background contributions. The signal contribution from $t\bar{t}$ events in the simulation is generated with the ALPGEN event generator [11] for a top-quark mass of 172.5 GeV, and

parton-shower development is simulated with PYTHIA [12]. A matching scheme is applied to avoid double-counting of partonic event configurations [13].

The background can be split into two components. The first is instrumental background, arising from multijet (MJ) production, where a jet with high electromagnetic fraction mimics an electron in the e+jets channel, or for μ +jets, where a muon contained within a jet is emitted in the decay of a heavy-flavor quark, and appears isolated. The physics background originates from processes with a final state similar to $t\bar{t}$ signal. The dominant background for the selected sample arises from W +jets production. Other physics backgrounds taken into account are from single top, diboson, and $Z \rightarrow \tau\tau$ production, and contributions from $Z \rightarrow \mu\mu$ ($Z \rightarrow ee$) in the μ +jets (e+jets) channel. These backgrounds are taken from Monte Carlo (MC) simulation normalized to the next-to-leading order (NLO) predictions. Diboson events (WW , WZ and ZZ) are generated with PYTHIA, single-top production with the COMPHEP generator [14], and Z +jets, with $Z \rightarrow ee$, $\mu\mu$ and $\tau\tau$, are simulated using ALPGEN. For the latter the Z boson p_T distribution is corrected to match the distribution observed in data, taking also into account the dependence on the jet multiplicity. All generated samples use CTEQ6L1 parton distributions (PDFs) [15].

The contribution from MJ background is estimated from data using the ‘‘Matrix Method’’ [16]. For the most important background in the ℓ +jets channel, namely W +jets, the normalization is derived from data but the shapes of the distributions are obtained from simulation. The W +jets sample consists of events where the W boson is produced through an electroweak interaction, and additional partons are generated through QCD processes. The W +jets samples are generated using ALPGEN, with parton showers developed through PYTHIA. The overall normalization of W +jets background is obtained as a function of jet multiplicity for each of the channels used in the analysis, by subtracting from data the physics backgrounds determined from MC, the expected $t\bar{t}$ signal and the MJ contribution obtained through the Matrix Method.

V. EFFICIENCIES AND YIELDS

Selection and tagging efficiencies for each of the ℓ +jets channels are summarized, together with their statistical uncertainties in Table I. We apply the same b -tagging algorithm both to data and to simulated events, but correct the simulation based on jet flavor, p_T , and η to achieve the same performance of the b -tagging algorithm as in data. These correction factors are determined from control samples in data, and used to predict the yield of $t\bar{t}$ events with 0, 1, or ≥ 2 b -tagged jets in data. We also correct lepton and jet identification and reconstruction efficiencies in simulation to match the ones measured in data.

decay mode	Channel	jets	preselection	= 1 tag	≥ 2 tags
$t\bar{t}j$	e+jets	= 3	0.101	0.472	0.174
	μ +jets		0.064	0.465	0.177
	e+jets	≥ 4	0.091	0.459	0.264
	μ +jets		0.062	0.461	0.260
$t\bar{t}ll$	e+jets	= 3	0.036	0.461	0.245
	μ +jets		0.022	0.458	0.251
	e+jets	≥ 4	0.008	0.464	0.254
	μ +jets		0.005	0.436	0.280

TABLE I: Preselection efficiencies and event tagging probabilities for lepton+jets and dilepton contributions to ℓ +jets channels. The statistical uncertainties on the efficiencies are of the order of 1-2%.

Tables II summarize the predicted background and observed number of events in the e+jets and μ +jets data with 0- 1- and ≥ 2 tags, together with the number of $t\bar{t}$ signal event candidates using the measured $t\bar{t}$ cross section in the b -tagging analysis.

VI. CROSS SECTION MEASUREMENT USING KINEMATIC INFORMATION

A. Discrimination

To discriminate the $t\bar{t}$ signal from the background, we construct a distribution that exploits differences between the kinematic properties of the $t\bar{t}$ ℓ +jets signal and the dominant W +jets background using the toolkit TMVA [17].

channel	sample	0 b -tags	1 b -tag	≥ 2 b -tags
e+3 jets	W +jets	2431 ± 134	245 ± 25	20 ± 4
	Multijet	400 ± 66	49 ± 8	4 ± 1
	Z +jets	158 ± 36	20 ± 6	2 ± 1
	Other	114 ± 17	29 ± 5	6 ± 1
	$t\bar{t}$	217 ± 26	302 ± 25	120 ± 14
	Total	3320 ± 113	645 ± 33	153 ± 16
	Observed	3316	648	154
e+ ≥ 4 jets	W +jets	319 ± 72	41 ± 10	5 ± 1
	Multijet	80 ± 14	15 ± 3	1 ± 0.2
	Z +jets	22 ± 6	4 ± 2	0.4 ± 0.2
	Other	18 ± 4	5 ± 1	1 ± 0.4
	$t\bar{t}$	134 ± 24	229 ± 32	136 ± 19
	Total	574 ± 49	294 ± 25	144 ± 19
	Observed	596	289	127
μ +3 jets	W +jets	1930 ± 82	185 ± 18	16 ± 3
	Multijet	54 ± 24	9 ± 4	0 ± 0
	Z +jets	134 ± 26	14 ± 4	2 ± 1
	Other	93 ± 13	23 ± 4	6 ± 1
	$t\bar{t}$	150 ± 16	206 ± 18	84 ± 10
	Total	2360 ± 65	437 ± 24	107 ± 11
	Observed	2364	426	114
μ + ≥ 4 jets	W +jets	306 ± 48	43 ± 7	6 ± 2
	Multijet	13 ± 6	4 ± 2	0 ± 0
	Z +jets	15 ± 4	2 ± 1	1 ± 0.5
	Other	14 ± 3	5 ± 1	2 ± 0.4
	$t\bar{t}$	102 ± 16	173 ± 21	102 ± 14
	Total	448 ± 35	227 ± 16	109 ± 14
	Observed	428	236	119

TABLE II: Yields for e+jets and μ +jets with 0-, 1- and ≥ 2 tags. The number of $t\bar{t}$ events is calculated using the cross section measured in the b -tagging analysis. Uncertainties include statistical and systematic contributions.

We split both the $t\bar{t}$ and the W +jets samples into two. One half is used for training and testing, and the other half for application in analysis. All other samples, including the dilepton part of $t\bar{t}$ decays, are considered for the cross section extraction step.

We use a boosted decision tree (BDT) [18] for distinguishing signal from background. The settings for the BDT are a “random forest” with 200 “trees”, with the “boosting” [19] type set to bagging, and the separation type set to the “Gini index” [20] without pruning.

We use variables that provide separation between signal and background, and also are described well by the MC simulation. To minimize the sensitivity to the modeling of soft radiation and the underlying event we use only up to five leading jets in calculating any variable. The variables are listed below.

Event aplanarity: The normalized momentum tensor \mathcal{M} is defined as:

$$\mathcal{M}_{ij} = \frac{\sum_o p_i^o p_j^o}{\sum_o |\vec{p}^o|^2}, \quad (1)$$

where \vec{p}^o is the momentum vector of a reconstructed object o , and i and j are Cartesian coordinates. The sum over objects includes jets and the selected lepton. The diagonalization of \mathcal{M} yields three eigenvalues $\lambda_1 \geq \lambda_2 \geq \lambda_3$, with $\lambda_1 + \lambda_2 + \lambda_3 = 1$.

The aplanarity \mathcal{A} is defined as $\mathcal{A} = \frac{3}{2}\lambda_3$, and reflects the isotropy of an event. \mathcal{A} ranges between 0 and 0.5. Large values correspond to spherical events, while small values correspond to planar events. While $t\bar{t}$ final states are more spherical, as is typical for decay of massive objects, W +jets and MJ events tend to be more planar.

Event sphericity: The sphericity is defined as $\mathcal{S} = \frac{3}{2}\lambda_2 + \frac{3}{2}\lambda_3$, and $t\bar{t}$ events therefore have greater \mathcal{S} than background events;

\mathbf{H}_T^ℓ : The scalar sum of the transverse momenta of the jets with highest p_T (H_T) and the transverse momentum of the lepton;

\mathbf{H}_T^3 : The scalar sum of the p_T of the third and fourth jet in an event. As these two jets come mainly from gluon radiation in the background W +jets sample but from W decays in the $t\bar{t}$ sample, \mathbf{H}_T^3 has higher values for the latter. This variable is only used in the electron and muon channels with at least three jets. For the events with exactly three jets \mathbf{H}_T^3 is the p_T of the third jet;

$\mathbf{M}_t^{\text{jet}}$: For the electron and muon channels with exactly 2 jets, instead of \mathbf{H}_T^3 , which is not defined with only 2 jets, the transverse mass of the dijet system is used;

$\mathbf{M}_{\text{event}}$: The invariant mass of the lepton, the neutrino and leading jets. The energy of the neutrino is determined constraining the invariant mass of lepton and neutrino to the mass of the W boson;

$\mathbf{M}_T^{\text{j}2\nu\ell}$: Transverse mass of the system consisting of the second leading jet, the lepton and the neutrino where the energy of the neutrino is determined as for M_{event} .

Figure 1 shows the distributions of selected discriminating variables in data compared to the sum of expected $t\bar{t}$ signal and background contributions for the combined $\ell + 4$ jets channel.

The output of the BDT discriminant is presented in Fig. 2.

B. Extraction of cross section

We perform a maximum likelihood fit to the BDT discriminants distributions to measure the $t\bar{t}$ cross section in the kinematical analysis. We use templates for dilepton and ℓ +jets contributions to $t\bar{t}$ signal, WW , WZ , ZZ , Z +jets, single top (s and t -channel), MJ and W +jets backgrounds in the μ +jets and e +jets final states. The likelihood function is defined as:

$$L(N_t^{t\bar{t}}, N_t^W, N_t^{MC}, N_t^{qcd}) = \left[\prod_i \mathcal{P}(n_i^o, \mu_i) \right] \mathcal{P}(N_{\ell-t}^o, N_{\ell-t}), \quad (2)$$

where $\mathcal{P}(n, \mu)$ denotes the Poisson probability density function for n observed events given an expectation value of μ and $N_t^{t\bar{t}}$, N_t^W , N_t^{MC} , N_t^{MJ} are the number of $t\bar{t}$, W +jets, MC background (diboson, single top, Z +jets) and MJ events in the selected sample, respectively. In the first term of Eq. 2, i runs over all bins of the discriminant; n_i^o is the content of bin i in the selected data sample, and μ_i is the expectation for bin i .

The negative of the log-likelihood function in Eq. 2 is minimized

$$-\log L(N_t^{t\bar{t}}, N_t^W, N_t^{MC}, N_t^{qcd}) \simeq \sum_i (-n_i^o \log \mu_i + \mu_i) - N_{\ell-t}^o \log N_{\ell-t} + N_{\ell-t}, \quad (3)$$

where any terms independent of the minimization parameters have been dropped. The MC backgrounds N_t^{MC} are determined from the theoretical cross sections, efficiency and luminosity. Since the systematics is allowed to float, the amount of this background can change. The fitted parameters ($N_t^{t\bar{t}}$, N_t^W and N_t^{MJ}) are given by their values at the minimum of the negative log-likelihood function, and their uncertainties are defined by a change in the negative log-likelihood by one-half of a unit at its minimum.

VII. CROSS SECTION MEASUREMENT WITH b -TAGGING

A. Discrimination

In the SM it is predicted that the top quark decays almost exclusively into a W boson and a b -quark ($t \rightarrow Wb$). Besides using kinematic information to discriminate the $t\bar{t}$ signal from the background, we can therefore enrich the fraction of $t\bar{t}$ events using b -jet identification. To measure the $t\bar{t}$ cross section, we split the sample into events with 0, 1 and ≥ 2 b -tagged jets. The W +jets events are normalized to the difference between data and signal and all other sources of background, before applying b -tagging. Figure 3 shows a comparison of the distributions in data with 0, 1 or ≥ 2 b -tagged jets with the SM $t\bar{t}$ cross section, and the contributions from the different backgrounds.

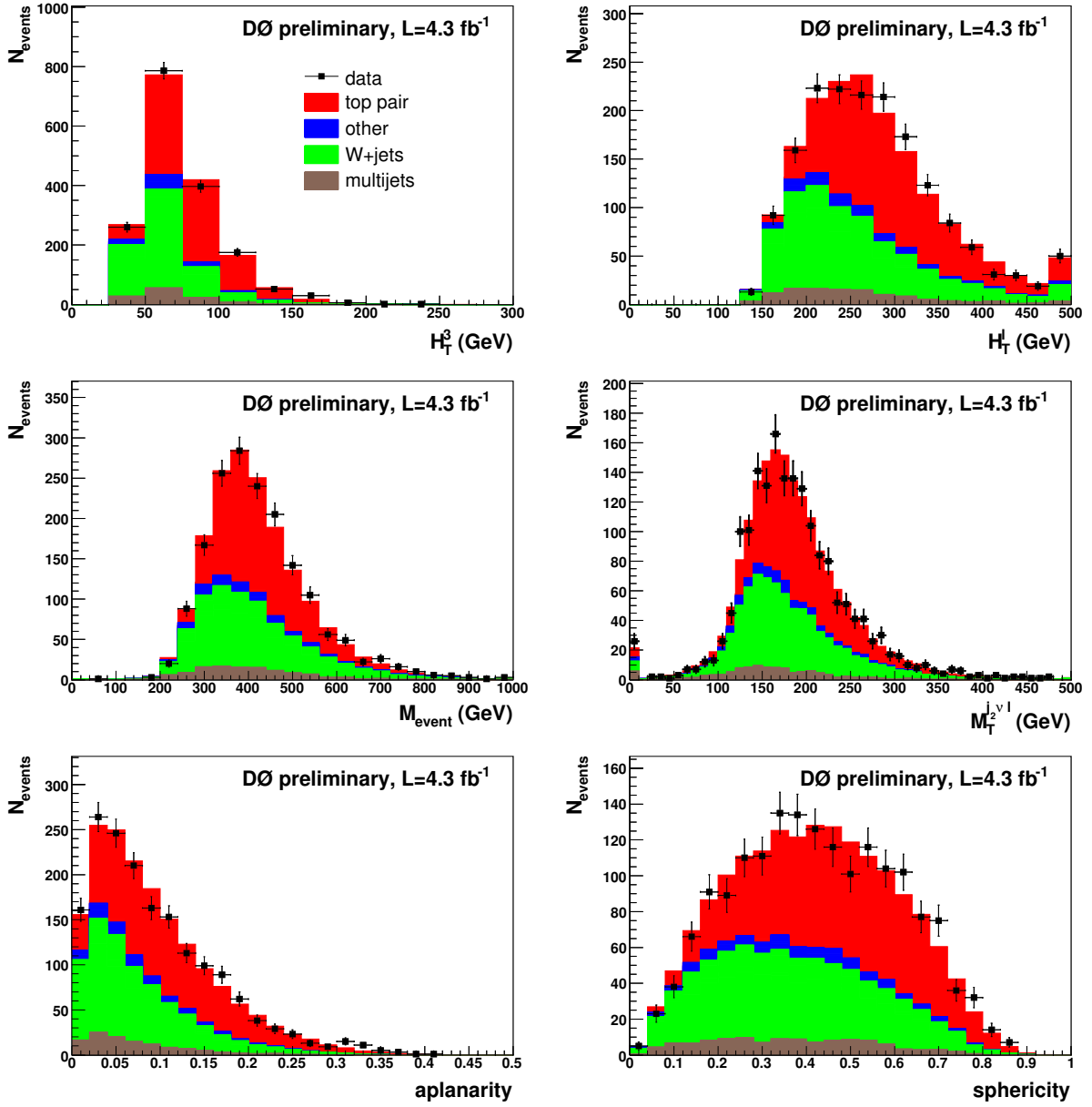


FIG. 1: Distributions of variables used as input to the BDT in data overlaid with the predicted background and expected $t\bar{t}$ signal for the $\ell+\geq 4$ jets channel.

B. Extraction of cross section

An iterative procedure is used to extract the $t\bar{t}$ cross section after b -tagging. Details of this method, as well as the general treatment of systematic uncertainties is described in detail in [21]. The fit of the $t\bar{t}$ cross section ($\sigma_{t\bar{t}}$) to data is performed using a maximum likelihood fit for the predicted number of events, which depends on $\sigma_{t\bar{t}}$. To take into account each channel, the likelihood maximization procedure multiplies the Poisson probabilities for all channels j :

$$\mathcal{L} = \prod_j \mathcal{P}(N_j^{\text{obs}}, N_j^{\text{predicted}}(\sigma_{t\bar{t}})) \quad (4)$$

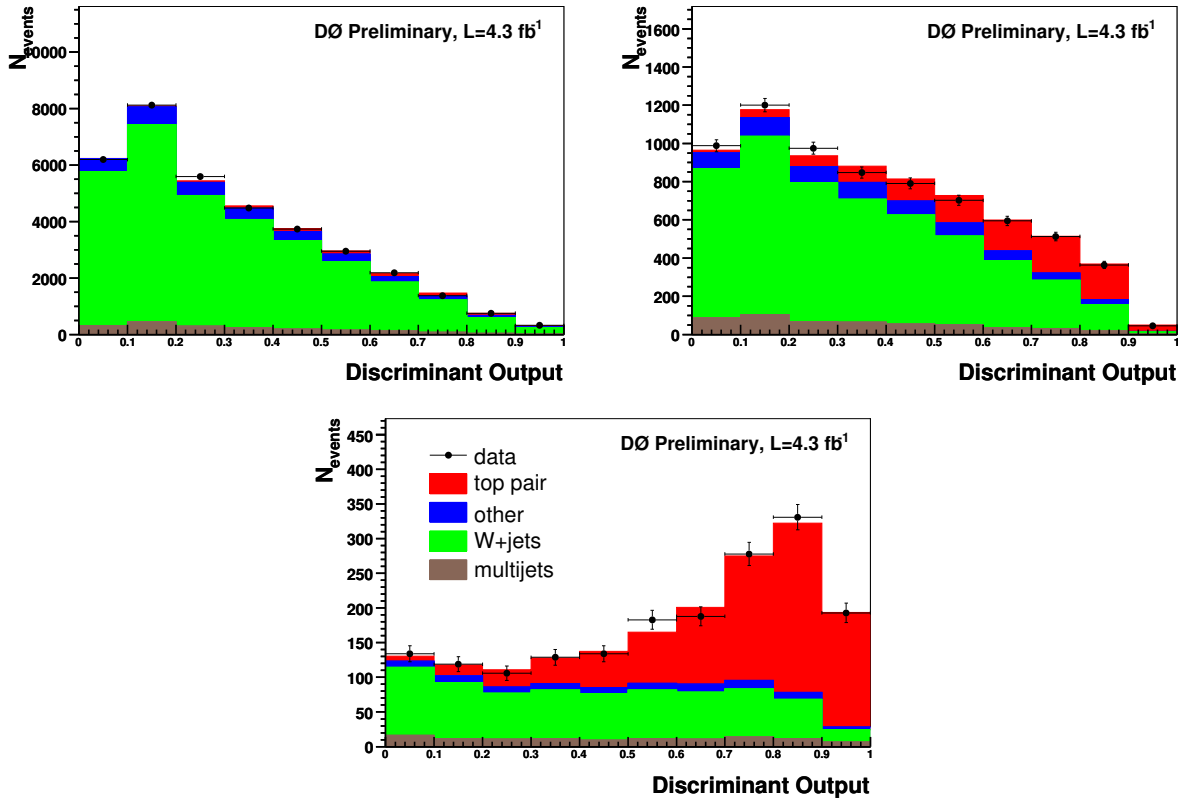


FIG. 2: Output of the BDT discriminant for $\ell+2$ jets (upper left), $\ell+3$ jets (upper right) and $\ell+\geq 4$ jets (lower), showing contributions from $t\bar{t}$ signal using a cross section of 7.70 pb and backgrounds.

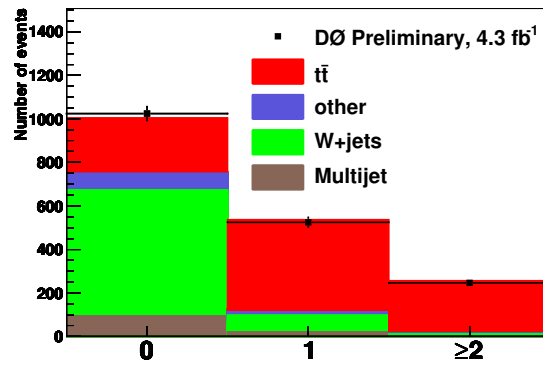


FIG. 3: Distribution of events with 0, 1 and ≥ 2 b -tagged jets for the combined ℓ +jets channels, showing contributions from $t\bar{t}$ signal using a cross section of 7.93 pb and backgrounds.

where $\mathcal{P}(N^{\text{obs}}; N^{\text{predicted}})$ defines the Poisson probability to observe N^{obs} events when the predicted number of events is $N^{\text{predicted}}$.

The systematic uncertainties are incorporated in the fit using nuisance parameters [22], each represented by a Gaussian term. The correlation of systematic uncertainties among channels is taken into account by assigning the same nuisance parameter to each correlated systematic [16].

VIII. SYSTEMATIC UNCERTAINTIES

Different sources of systematic uncertainty can affect the preselection efficiencies, the b -tagging probabilities and the distributions of variables used to build the kinematical discriminant. The uncertainty on integrated luminosity is 6.1% [23]. This affects the yields of signal and backgrounds estimated from simulation in a similar way and is used as additional nuisance parameter on the selection efficiency of each contribution.

Sources of uncertainty that affect the preselection efficiency are: data-quality requirements, electron- and muon-identification efficiencies, electron and muon trigger efficiencies, modeling of additional $p\bar{p}$ collisions in the MC simulation, corrections on the longitudinal distribution of the PV in the MC simulation, efficiency of the PV selection, limited MC statistics, uncertainties on cross sections used in MC and for decay branching ratios of the top quarks, uncertainties on the simulation of the p_T distribution of the Z , b -fragmentation, PDF and modeling of the signal. The sources of uncertainties that affect b -tagging involve corrections on the b , c and light-flavor jets tagging rates, requirements on jets to be usable for tagging and on the calorimeter response to b jets.

The uncertainties on MJ background from the Matrix Method are propagated to the yields of MJ background. Additionally the limited statistics of events folded into the analysis to model MJ background is taken into account, as are uncertainties on the flavor composition of W +jets and Z +jets processes.

Uncertainties on the jet energy scale, jet energy resolution, jet reconstruction and identification efficiency and vertex requirements on jets affect preselection, b -tagging efficiency and the discriminant distribution. Additionally, the latter is affected by the limited statistics of templates. The general treatment of uncertainties on kinematical discriminant templates is described in [21] In Table III, correlated (indicated by “X”) and uncorrelated systematics are indicated for completeness.

IX. RESULTS

A. Kinematical method

The extraction of $\sigma_{t\bar{t}}$ is performed using the nuisance parameter method of Ref. [16] that allows systematic uncertainties to influence the result of the fit. Each independent source of systematics is modeled as a free parameter, with the constraint of a Gaussian of mean at zero and width of unity, floated during the optimization procedure. All results are provided for a top-quark mass of 172.5 GeV. Since the kinematical discriminant has a background-dominated region, fitting the $t\bar{t}$ cross section, while allowing each individual source of systematic uncertainty float, can result in an improved total uncertainty. Table IV shows the measured cross section in e+jets, μ +jets and for the combined ℓ +jets channel. Table V shows the corresponding uncertainties.

To check the consistency of these results, pseudo-experiments have been performed. We generated 10,000 ensembles representing the data sample but varied the number of expected signal and background events for each ensemble within a Poisson statistics. In addition the nuisance parameters for each individual source of systematic uncertainty are varied using a Gaussian function. All systematic uncertainties and their correlations are taken into account. As a measure of the consistency, we calculate the probability that the absolute value of the difference between the measured cross sections in the e+jets and μ +jets channels are as given in Tab. IV or larger. The two measurements are consistent at the level of 9%.

B. b -tagging method

In Table VI results are presented for the fits in the e+jets, μ +jets, and combined ℓ +jets channels, and Table VII gives the systematic uncertainties.

To check the consistency of these results, pseudo-experiments have been performed in the same way as described in the previous section yielding the consistency between the measured cross sections in the e+jets and μ +jets channels as given in Tab. VI of 21%.

X. CONCLUSION

We have measured the $t\bar{t}$ production cross section in the $\ell(e, \mu)$ +jets final states using two analysis techniques, in 4.3 fb^{-1} of data collected with the D0 detector. For a top quark mass of 172.5 GeV, we obtain:

$$\sigma_{t\bar{t}} = 7.70_{-0.70}^{+0.79} \text{ (stat + syst + lumi) pb,}$$

Systematic	e+jets	μ +jets
Correlated between channels		
Jet ID	X	X
Jet energy scale	X	X
Jet energy resolution	X	X
Taggability	X	X
Electron ID	X	
Muon ID		X
Muon track		X
Muon isolation		X
Data quality	X	X
$\Delta z(l, PV)$	X	X
Primary vertex	X	X
Vertex confirmation	X	X
PDF	X	X
signal modeling	X	X
Color Reconnection	X	X
ISR/FSR	X	X
W +jets heavy flavor scale factor	X	X
Z +jets heavy flavor scale factor	X	X
b -fragmentation	X	X
b -Jet energy scale	X	X
Lumi reweighting	X	X
$p_T(Z)$ reweighting	X	X
b - c -tag SFs	X	X
fake tag rate	X	X
Integrated luminosity	X	X
background cross sections	X	X
branching fractions	X	X
Uncorrelated		
ℓ +jets trigger	X	X
Monte Carlo statistics	X	X
Template statistics	X	X
Statistics in loose–tight	X	X
ϵ_{qcd} in μ +jets		X
ϵ_{qcd} in e+jets	X	
ϵ_{signal} in μ +jets		X
ϵ_{signal} in e+jets	X	

TABLE III: Summary of systematic uncertainties in each channel and the correlations between the systematics.

channel	$\sigma_{t\bar{t}}$ [pb]
e+jets	$6.53^{+0.79}_{-0.69}$ (stat+syst+lumi)
μ +jets	$8.37^{+1.08}_{-0.93}$ (stat+syst+lumi)
ℓ +jets	$7.70^{+0.79}_{-0.70}$ (stat+syst+lumi)

TABLE IV: Measured $t\bar{t}$ production cross section using kinematical information for separate channels derived with the nuisance parameter fit. Uncertainties include statistical and systematic contributions.

using kinematic event information and

$$\sigma_{t\bar{t}} = 7.93^{+1.04}_{-0.91} \text{ (stat + syst + lumi) pb,}$$

using b -jet identification to separate signal and background. Both results are in agreement and consistent with the theoretical predictions of $7.46^{+0.48}_{-0.67}$ pb ([1]) based on the full NLO matrix element including soft-gluon resummation at NNLO logarithmic accuracy.

Summary of nuisance parameter likelihood with systematics on cross section			
Source	Offset	$+\sigma$	$-\sigma$
Statistical only	+7.05	+0.32	-0.32
Event preselection	+0.02	+0.13	-0.12
Muon identification	-0.03	+0.07	-0.05
Electron identification and smearing	+0.21	+0.18	-0.16
Luminosity reweighting	+0.00	+0.02	+0.00
$p_T(Z)$ reweighting	+0.01	+0.02	+0.00
signal modeling	-0.14	+0.14	-0.13
Color reconnection	-0.01	+0.05	-0.04
ISR/FSR variation	-0.00	+0.00	+0.00
EM triggers	-0.00	+0.00	+0.00
Muon triggers	-0.12	+0.12	-0.11
Jet energy scale	+0.21	+0.00	+0.00
Vertex confirmation	-0.20	+0.07	-0.04
b-Jet energy scale	-0.00	+0.03	-0.01
Jet energy resolution	+0.60	+0.07	-0.06
Jet reconstruction and identification	-0.08	+0.08	-0.07
b fragmentation	-0.03	+0.08	-0.07
Matrix method ϵ_{QCD} and ϵ_{sig}	-0.07	+0.00	+0.00
Monte Carlo background x-section	+0.01	+0.00	-0.01
Monte Carlo signal & bkg branching ratio	+0.00	+0.07	-0.05
Monte Carlo bkg scale factors	+0.05	+0.03	-0.01
Monte Carlo statistics	+0.00	+0.04	-0.02
W fractions matching + higher order effects	+0.08	+0.04	-0.04
PDF	+0.01	+0.09	-0.07
Luminosity	+0.30	+0.50	-0.43
Event statistics for matrix method	-0.00	+0.01	+0.00
Total systematics (quad sum of the above)	+0.82	+0.62	+0.53
Total error (nuisance parameter fit)	7.70	+0.79	-0.70

TABLE V: Result of nuisance parameter fit and listing of separate uncertainties for the ℓ +jets channels combined for the kinematical $t\bar{t}$ cross section, with the listing of the individual sources of systematics. The offset shows how the mean value of the measured cross section is shifted due to the respective source of systematics. $\pm\sigma$ gives the impact on the measured cross section when a source of systematics is varied up and down within 1 s.d. of its error.

channel	$\sigma_{t\bar{t}}[\text{pb}]$
e +jets	$7.41^{+1.07}_{-0.96}$ (stat+syst+lumi)
μ +jets	$8.60^{+1.27}_{-1.06}$ (stat+syst+lumi)
ℓ +jets	$7.93^{+1.04}_{-0.91}$ (stat+syst+lumi)

TABLE VI: Measured $t\bar{t}$ production cross section using b -tagging derived with the nuisance parameter method for each individual channel. Uncertainties include statistical and systematic contributions.

Acknowledgments

We thank the staffs at Fermilab and collaborating institutions, and acknowledge support from the DOE and NSF (USA); CEA and CNRS/IN2P3 (France); FASI, Rosatom and RFBR (Russia); CNPq, FAPERJ, FAPESP and FUNDUNESP (Brazil); DAE and DST (India); Colciencias (Colombia); CONACyT (Mexico); KRF and KOSEF (Korea); CONICET and UBACyT (Argentina); FOM (The Netherlands); STFC and the Royal Society (United Kingdom); MSMT and GACR (Czech Republic); CRC Program and NSERC (Canada); BMBF and DFG (Germany); SFI (Ireland); The Swedish Research Council (Sweden); and CAS and CNSF (China).

Summary of nuisance parameter likelihood with systematics on cross section			
Source	Offset	$+\sigma$	$-\sigma$
Statistical only	+7.83	+0.28	-0.28
Event preselection	-0.00	+0.14	-0.13
Muon identification	-0.06	+0.07	-0.07
Electron identification and smearing	+0.24	+0.18	-0.17
Luminosity reweighting	-0.00	+0.02	+0.00
$p_T(Z)$ reweighting	-0.00	+0.00	-0.00
signal modeling	+0.11	+0.16	-0.15
Color reconnection	-0.01	+0.07	-0.06
ISR/FSR variation	-0.00	+0.00	-0.03
EM triggers	+0.03	+0.06	-0.06
Muon triggers	-0.20	+0.13	-0.12
Jet energy scale	+0.08	+0.12	-0.12
Vertex confirmation	+0.07	+0.22	-0.21
b-Jet energy scale	+0.00	+0.04	-0.04
Jet energy resolution	-0.01	+0.02	-0.02
Jet reconstruction and identification	+0.04	+0.12	-0.11
Taggability in data	-0.01	+0.10	-0.09
b-tag TRF	-0.21	+0.33	-0.32
c-tag TRF	+0.00	+0.00	+0.00
light tag TRF	-0.01	+0.10	-0.11
b fragmentation	+0.00	+0.02	-0.02
Matrix method ϵ_{QCD} and ϵ_{sig}	+0.01	+0.04	-0.04
Monte Carlo background x-section	-0.00	+0.02	-0.02
Monte Carlo signal & bkg branching ratio	-0.00	+0.07	-0.07
Monte Carlo bkg scale factors	-0.00	+0.04	-0.04
Monte Carlo statistics	-0.01	+0.12	-0.12
PDF	-0.00	+0.19	-0.17
Luminosity	-0.02	+0.53	-0.46
Event statistics for matrix method	-0.00	+0.06	-0.06
Total systematics (quad sum of the above)	-0.04	+0.84	+0.77
Total error (nuisance parameter fit)	7.93	+1.04	-0.91

TABLE VII: Measured $t\bar{t}$ production cross section with b -tagging using the nuisance parameter method for ℓ +jets channels combined, with the listing of the individual sources of systematics. The offset shows how the mean value of the measured cross section is shifted due to the respective source of systematics. $\pm\sigma$ gives the impact on the measured cross section when a source of systematics is varied up and down within 1 s.d. of its error.

- [2] N. Kidonakis and R. Vogt, Phys. Rev. D **68**, 114014 (2003).
- [3] M. Cacciari, S. Frixione, M. L. Mangano, P. Nason and G. Ridolfi, JHEP **0404**, 068 (2004)
- [4] V. M. Abazov *et al.* [D0 Collaboration], Nucl. Instrum. Meth. A **565**, 463 (2006)
- [5] Rapidity y and pseudorapidity η are defined as functions of the polar angle θ and parameter β as $y(\theta, \beta) \equiv \frac{1}{2} \ln [(1 + \beta \cos \theta)/(1 - \beta \cos \theta)]$ and $\eta(\theta) \equiv y(\theta, 1)$, where β is the ratio of a particle's momentum to its energy.
- [6] Impact parameter is defined as the distance of closest approach (d_{ca}) of the track to the primary vertex in the plane transverse to the beamline. Impact parameter significance is defined as $d_{ca}/\sigma_{d_{ca}}$, where $\sigma_{d_{ca}}$ is the uncertainty on d_{ca} .
- [7] V. Abazov *et al.*, FERMILAB-PUB-05-034-E (2005).
- [8] V. M. Abazov *et al.* [D0 Collaboration], Phys. Rev. Lett. **100**, 192004 (2008)
- [9] V. M. Abazov *et al.* [D0 Collaboration], Phys. Rev. D **76**, 092007 (2007).
- [10] V. M. Abazov *et al.* [D0 Collaboration], *b-Jet Identification in the D0 Experiment*, arXiv:1002.4224 [hep-ex].
- [11] M. L. Mangano, M. Moretti, F. Piccinini, R. Pittau and A. D. Polosa, JHEP **0307**, 001 (2003)
- [12] T. Sjöstrand, L. Lonnblad, S. Mrenna, PYTHIA6.3 *physics and manual*, hep-ph/0308153 (2003).
- [13] M. L. Mangano, M. Moretti, F. Piccinini, and M. Treccani, J. High Energy Phys. 01 (2007) 013.
- [14] E.Boos *et al.*, [CompHEP Collaboration], Nucl. Instrum. Meth. A534 (2004) 250.
- [15] J. Pumplin *et al.*, JHEP 0207, 012(2002).
- [16] V. M. Abazov *et al.* [D0 Collaboration], Phys. Rev. D **74**, 112004 (2006).
- [17] A. Hoecker *et al.*, *TMVA - Toolkit for Multivariate Data Analysis*, arXiv:physics/0703039.
- [18] J. M. Campbell and R. K. Ellis, Phys. Rev. D **65**, 113007 (2002)
- [19] Y. Freund and R. E. Schapire, in *Machine Learning: Proceedings of the Thirteenth International Conference*, edited by

- L. Saitta (Morgan Kaufmann, San Francisco, 1996), p. 148.
- [20] C. Gini, *Variabilità e Mutabilità* (1912), reprinted in *Memorie di Metodologica Statistica*, edited by E. Pizetti and T. Salvemini (Libreria Eredi Virgilio Veschi, Rome, 1955).
- [21] V. M. Abazov *et al.* [D0 Collaboration], [arXiv:0801.1326 [hep-ex]]
- [22] P. Sinervo, in *Proceedings of Statistical Methods in Particle Physics, Astrophysics, and Cosmology*, edited by L. Lyons, R. P. Mount, and R. Reitmeyer (SLAC, Stanford, 2003), p. 334.
- [23] T. Andeen *et al.*, FERMILAB-TM-2365 (2007).